

<https://helda.helsinki.fi>

---

## Nutrient availability as major driver of phytoplankton-derived dissolved organic matter transformation in coastal environment

Asmala, Eero

2018-01

---

Asmala , E , Haraguchi , L , Jakobsen , H H , Massicotte , P & Carstensen , J 2018 , ' Nutrient availability as major driver of phytoplankton-derived dissolved organic matter transformation in coastal environment ' , Biogeochemistry , vol. 137 , no. 1-2 , pp. 93-104 . <https://doi.org/10.1007/s10533-017-0403-0>

---

<http://hdl.handle.net/10138/307042>

<https://doi.org/10.1007/s10533-017-0403-0>

---

cc\_by

acceptedVersion

---

*Downloaded from Helda, University of Helsinki institutional repository.*

*This is an electronic reprint of the original article.*

*This reprint may differ from the original in pagination and typographic detail.*

*Please cite the original version.*

**Nutrient availability as major driver of phytoplankton-derived dissolved organic matter transformation in coastal environment**

Authors: \*Asmala, Eero<sup>1</sup>; Haraguchi, Lumi<sup>1</sup>; Jakobsen, Hans H. <sup>1</sup>; Massicotte, Philippe<sup>2</sup>; Carstensen, Jacob<sup>1</sup>

<sup>1</sup> Department of Bioscience, Aarhus University, Roskilde, Denmark

<sup>2</sup> Takuvik Joint International Laboratory, Université Laval & Centre National de la Recherche Scientifique, Québec, Canada

**Correspondence:**

Dr. Eero Asmala

University of Helsinki, Tvärminne Zoological Station

J.A. Palménin tie 260, 10900 Hanko, Finland

eero.asmala@helsinki.fi, +3584578722010, ORCID: 0000-0002-9150-1227

## Abstract

Incubation experiments were performed to examine the processing of fresh autochthonous dissolved organic matter (DOM) produced by coastal plankton communities in spring and autumn. The major driver of observed DOM dynamics was the seasonally variable inorganic nutrient status and characteristics of the initial bulk DOM, whereas the characteristics of the phytoplankton community seemed to have a minor role. Net accumulation of dissolved organic carbon (DOC) during the 18-d experiments was 3.4 and 9.2  $\mu\text{mol l}^{-1} \text{ d}^{-1}$  in P-limited spring and N-limited autumn, respectively. Bacterial bioassays revealed that the phytoplankton-derived DOC had surprisingly low proportions of biologically labile DOC, 12.6 % (spring) and 17.5 % (autumn). The optical characteristics of the DOM changed throughout the experiments, demonstrating continuous heterotrophic processing of the DOM pool. However, these temporal changes in optical characteristics of the DOM pool were not the same between seasons, indicating seasonally variable environmental drivers. Nitrogen and phosphorus availability is likely the main driver of these seasonal differences, affecting both phytoplankton extracellular release of DOM and its heterotrophic degradation by bacteria. These findings underline the complexity of the DOM production and consumption by the natural planktonic community, and show the importance of the prevailing environmental conditions regulating the DOM pathways.

**Keywords:** extracellular release; autochthonous organic matter; carbon cycling; colored dissolved organic matter

## 1. Introduction

Dissolved organic matter (DOM) in the marine environment is a key component in the global carbon cycle (Carlson & Hansell 2014). DOM provides a carbon source for heterotrophic metabolism, but also affects the underwater light regime because the colored fraction of the DOM pool (CDOM) absorbs both UV and visible light. The optical properties of DOM (absorbance and fluorescence) have been widely used to determine the origin and fate of DOM, as they are linked to the inherent chemical characteristics of the DOM pool (Weishaar et al. 2003; Osburn & Stedmon 2011; Reader et al. 2015). Studies on DOM absorbance and fluorescence have revealed significant biogeochemical processing of the DOM pool in coastal environments (Moran et al. 2000; Boyd & Osburn 2004). One of the major sources of DOM is the autochthonous production by phytoplankton (Søndergaard et al. 2000; Stedmon & Markager 2005). DOM is released from phytoplankton by multiple mechanisms such as excretion, exudation and cell lysis (Thornton 2014). In general, a major part of this DOM is extracellular release (ER) of dissolved organic carbon (DOC) compounds with little or no macronutrients (Mykkestad 1995). The transformation and consumption by heterotrophic organisms is altering the composition of this DOM pool rapidly after its release (Rochelle-Newall and Fisher 2002; Yamashita & Tanoue 2004; Romera-Castillo et al. 2011; Danhiez et al. 2017). The heterotrophic processing of natural DOM has been suggested to follow a reactivity continuum, where the most labile fractions are utilized first by heterotrophs, resulting in continuously increasing recalcitrance of the DOM pool (Vähätalo et al. 2010). However, our understanding of how ER is processed and transformed by the natural planktonic community and how it aligns with the reactivity continuum concept is limited. Further, there are significant gaps in our knowledge about the role of the seasonality on DOM – phytoplankton interactions.

The overall aim of this study was to quantify and characterize the transformation of the DOM originating from natural community of planktonic primary producers and bridge the knowledge gap between the extracellular release of dissolved organic carbon and optical properties of DOM in coastal waters. Specifically, we wanted to examine changes in DOM optical characteristics related to phytoplankton primary production in changing inorganic nutrient conditions. We hypothesize that 1) extracellular release of DOM as a result of phytoplankton primary production is rapidly reworked by heterotrophic processing and 2) these transformation processes vary seasonally, depending on the phytoplankton community

and nutrient availability. To test these hypotheses, changes in DOM quantity and quality were studied in two laboratory experiments with natural coastal plankton communities collected in spring and in the autumn including manipulations of nutrient conditions.

## **2. Material & methods**

### **2.1. Experimental setup**

We sampled water from Roskilde Fjord (Denmark), a shallow fjord-like temperate estuary in the coastal Baltic Sea, with small freshwater inputs and a long freshwater residence time (Flindt et al. 1997). Despite the relatively high nutrient inputs from the agriculture-dominated catchment, the system is net heterotrophic on an annual scale (Staehr et al. 2017).

Experiments were designed to cover periods that are expected to be prominently autotrophic (March) and heterotrophic (September) (Staehr et al. 2017). Typically, the highest levels of net ecosystem production are observed during the phytoplankton spring bloom that occurs in March-April, after which the chlorophyll levels stay moderate throughout the growth season (Staehr et al. 2017). Water for the experiments was sampled from the surface at 55.71 N, 12.07 E on 14 September 2015 and 14 March 2016. Samples were pre-screened with 100  $\mu\text{m}$  mesh, transferred into HDPE carboys and transported to the laboratory within 1 h.

Incubations were carried out for 18 days, using six 10 L glass bottles, which were filled with sample water. Three of the replicate units were spiked with 3  $\mu\text{mol l}^{-1}$  of  $\text{NO}_3^-$ -N (as  $\text{NaNO}_3$ ) on first four days of the experiments, totaling an addition of 12  $\mu\text{mol N l}^{-1}$ , and three units were controls. Experiment units were incubated at  $10 \pm 1$  °C in a climate-controlled room, with daylight fluorescent tubes on a 16:8 light: dark cycle in saturated PAR light at an irradiance of 100–120  $\mu\text{mol m}^{-2} \text{s}^{-1}$ , measured just outside experimental bottles by a calibrated LI-193 spherical quantum sensor. Each bottle was placed on top of a magnetic stir plate, and constantly gently stirred with a teflon-coated magnetic bar. Samples were taken on five occasions during the 18-d incubations. Samples for DOM analyses were filtered with precombusted (450°C for 4 h) glass-fiber filters with a nominal pore size of 0.7  $\mu\text{m}$ .

To quantify the proportion of bioavailable (labile) fraction of DOC (BDOC), we conducted bacterial DOM degradation bioassays throughout the phytoplankton growth experiment. Samples for bioassays were filtered with non-combusted glass-fiber filters (nominal pore size 0.7  $\mu\text{m}$ ) and transferred into 250 ml glass bottles with gas-tight septum caps. To ensure replete nutrient conditions, bacterial bioassays were spiked with both nitrate-N ( $\text{NaNO}_3$ ) and

phosphate-P ( $\text{KH}_2\text{PO}_4$ ) of additional  $10 \mu\text{mol l}^{-1}$  and  $2 \mu\text{mol l}^{-1}$ , respectively. Bioassays were incubated in dark at room temperature ( $21 \pm 2^\circ\text{C}$ ) for 14 days. After the incubations, samples for DOM analysis were filtered with precombusted glass fiber filters. Samples for DOC were stored frozen until analysis whereas samples for CDOM and fluorescent dissolved organic matter (FDOM) samples were stored refrigerated until analysis.

## **2.2. Laboratory analyses**

The samples were analyzed for ammonium, nitrite, nitrate (DIN) and phosphate (DIP) using the techniques described by Hansen and Koroleff (2007). DOC was measured with a Shimadzu TOC-V<sub>CPH</sub> analyzer, and the accuracy of measured DOC concentrations was controlled by analyzing a seawater reference standard provided by the CRM (consensus reference material) program. CDOM absorption was measured using a Shimadzu 2401PC spectrophotometer with 5 cm quartz cuvette over the spectral range from 200 to 800 nm with 1 nm intervals. Ultrapure water was used as the blank for all samples. Excitation-emission matrices (EEMs) of fluorescent DOM (FDOM) were measured with a Varian Cary Eclipse fluorometer (Agilent). A blank sample of ultrapure water was removed from EEMs, as well as the scattering bands. EEMs were corrected for inner filter effects with absorbance spectra (Murphy et al. 2010) and Raman calibrated by normalizing to the area under the Raman scatter peak (excitation wavelength of 350 nm) of an ultrapure water sample run on the same session as the samples. Chl  $\alpha$  was determined from the combusted glass fiber filters, extracted with 10 ml ethanol (96%) for 24 hours in the dark, according to Holm-Hansen & Riemann (1978). Extracts were then stored in  $-20^\circ\text{C}$  freezer until measurement with an AU 10 Turner field fluorometer (Turner Designs, US). Phytoplankton was quantified under a size-calibrated inverted microscope (Nikon TI-U, Nikon Instruments Europe B.V.) following (Hasle 1978). Samples were fixed with acidic lugol's solution (2-4% final concentration) and sedimented in 10-50 ml Utermöhl chambers (Utermöhl 1958), depending on the cell density. Larger organisms ( $>30 \mu\text{m}$ ), including ciliates, were usually screened under lower magnification (100X) and the screened area depended on the density of the most abundant organisms, whereas smaller organisms ( $<30 \mu\text{m}$ ) were counted under higher magnification (200X and 400X). The organisms were grouped into larger taxonomical division aiming to evaluate the previously linkages between phytoplankton taxonomy and the quantity and quality of DOM (Aluwihare & Repeta 1999; Sarmiento et al. 2013).

### 2.3. Statistical analyses

To quantify the DOM optical characteristics, DOC-normalized absorbance at 254 nm ( $S_{254}$ ; Weishaar et al. 2003) and spectral slope coefficient between 275–295 nm ( $S_{275-295}$ ; Helms et al. 2008) were calculated. For assessing the terrestrial signature and the initial quality of the DOM pool, fluorescence metrics as peaks (Coble 1996), humification index (HIX) (Zsolnay et al. 1999) and biological index (BIX) (Huguet et al. 2009) were calculated from the measured and corrected EEMs. Processing of the EEMs was done using the eemR package for R software (Massicotte 2016). In order to resolve the “fingerprints” of the different DOM sources (autochthonous vs. allochthonous), we used the parallel factor analysis (PARAFAC) to distinguish different components of the measured and corrected EEMs (Murphy et al. 2008). PARAFAC modeling was done following the protocol by Murphy et al. (2013). Successive models from four to nine components were fitted using the DrEEM Matlab toolbox. Based on split-half analysis, a model with nine components was found to adequately model the fluorescence variability over the samples ( $R^2 = 0.9992$ ). The identified components were compared to previously validated components using the OpenFluor fluorescence database (<http://www.openfluor.org/>) and main characteristics are presented in Table S1 and Fig. S1. Note that PARAFAC was performed on a dataset with additional samples from Roskilde Fjord ( $n = 246$ ), which were processed in identical way as the experimental samples ( $n = 94$ ). This approach allows more accurate distinction of the components originating from the phytoplankton growth.

Measured DOM variables as well as DIN, DIP and Chl  $\alpha$  measurements were subjected to repeated-measures analysis using a mixed model in SAS (version 9.3). Variables were normalized by subtraction of the initial value to make the two seasonal experiments comparable. Fixed effects and variance components were estimated by restricted maximum-likelihood. The fixed effects in the model were season ( $s_i$ ), treatment ( $t_j$ ) and their two-way interaction ( $s_i \times t_j$ ) as well as the day of the experiment nested within season ( $d_k(s_i)$ ) and its interaction with treatment ( $d_k(s_i) \times t_j$ ), i.e.  $d_k(s_i)$  described the temporal trend for each season common to both treatments and  $d_k(s_i) \times t_j$  described the treatment-specific trends for each of the two seasons. A first-order autoregressive model was chosen for the error structure to describe temporal correlation within each experimental unit. Complete list of results is presented in Table 2. For revealing the temporal patterns in the multivariate DOM characteristics during the experiments, we conducted a principal component analysis (PCA)

separately on spectral CDOM absorbance (250–450 nm at 5 nm intervals) and on the nine FDOM components from the PARAFAC analysis. The DOM variables were normalized to initial conditions, which allows that the PC scores from the two seasons could be compared directly. Consequently, we examined if time trajectories of the PC scores differed between the two seasons, indicating different patterns of DOM processing during the experiments. Non-parametric Kruskal–Wallis test was used to examine the significance of treatment and season in observed BDOC values.

### 3. Results

The initial inorganic nutrient conditions were very different between the experiments (Fig. 1). In spring phosphorus was the potential growth limiting nutrient and nitrogen was potentially limiting in autumn (DIN:DIP ratios 52.5 and 0.93, respectively). In the beginning of the incubations, Chl  $\alpha$  increased during the first 4 days for both seasons and treatments. In the spring units (Fig. 2a–b), the first peak in Chl  $\alpha$  occurred at around day 4, after which the Chl  $\alpha$  started to decline for both treatments (nitrate added and control units), and a second peak emerged after day 12, reaching approximately same level as the first peak. The variation among units gradually increased during the spring experiment. In autumn experiment, the peak Chl  $\alpha$  was observed on day 8, after which the Chl  $\alpha$  declined rapidly to the same level in both treatments on day 14. Overall, Chl  $\alpha$  in units with nitrate addition was higher than in control units during the autumn experiment. In the beginning of the both seasons, the phytoplankton community was initially dominated by cryptophytes which were overcome by diatoms midway through the experiments (Fig. 2c–f).

The DOM pool in the beginning of the experiments was different between seasons (Table 1). DOC concentration was slightly lower in spring compared to autumn (465 and 499  $\mu\text{mol l}^{-1}$ , respectively), whereas DOM quality indicators, that can be used as proxies for allochthonous (terrestrial) vs. autochthonous, showed more pronounced allochthonous DOM signal in spring. This was signified by higher specific UV absorbance ( $\text{SUVA}_{254}$ ), lower slope coefficient ( $S_{275-295}$ ), higher humic-like fluorescence (peak C) and humification index (HIX). Conversely, the inverse patterns for these DOM characteristics and additionally higher values for protein-like fluorescence (peak T) and biological index (BIX) indicate stronger autochthonous contribution to the DOM pool in autumn.



DOC accumulation changed significantly over time ( $d_k(s_i)$ ) during the two experiments ( $F_{6, 21} = 30.3$ ,  $P < 0.0001$ ). Differences between nutrient added and control units were not significant in either experiment ( $F_{6, 21} = 1.14$ ,  $P = 0.37$ ). During the spring experiment, there was an increase in DOC concentration until day 7, after which there were only minor changes. In the autumn experiment, there was an initial decrease in DOC concentration, but after day 8, a large increase was observed. Nutrient additions had no effect on the DOC dynamics in the spring experiment, consistent with similar phytoplankton growth patterns among units (Fig. 1). On the other hand, at the end of the autumn experiment, DOC concentrations increased more with nitrate added. On average, the DOC increase during the 18-d incubations was  $62 \pm 40 \mu\text{mol l}^{-1}$  (13%) in the spring experiment, compared to  $165 \pm 30 \mu\text{mol l}^{-1}$  (33%) in autumn experiment (Fig. 4). Normalized to average chlorophyll concentrations, accumulation of DOC ( $\mu\text{g}/\mu\text{g}$ ) for spring and autumn was  $42 \pm 27$  and  $597 \pm 209 \text{ l}^{-1}$ , respectively. Assuming constant accumulation rates, the DOC increase was 3.4 and  $9.2 \mu\text{mol l}^{-1} \text{ d}^{-1}$  in spring and autumn, respectively. Effect of nitrate addition on DOC accumulation was not significant for either season.

The proportion of bioavailable (labile) fraction of the phytoplankton-derived DOC (BDOC) with dark-incubated bioassays varied between 1.1% and 44% (Fig. 3). For both seasons, BDOC from units with  $\text{NO}_3^-$  addition was not different from the control units. DOC from autumn units yielded higher BDOC values compared to that of the spring units, on average 17.5 and 12.6 %, respectively.

There was an increase of colored dissolved organic matter (CDOM) throughout the absorption spectrum during the spring experiment (Fig. 4). Interestingly, there was a loss during the autumn experiment across all wavelengths, despite the increasing DOC. The relative changes were more pronounced at higher wavelengths compared to lower wavelengths (+4% and -6% at 250 nm in spring and autumn, respectively, versus +72% and -16% at 400 nm).

As described in Table 1, the initial DOM composition was different between seasons. Also the dynamics of the DOM characteristics were different between experiments (Fig. 5). CDOM absorption at 254 nm ( $a_{\text{CDOM254}}$ ) decreased during the first days in the spring experiment (Fig. 5a), and increased again until midway of the experiment, after which there were no significant changes. In autumn,  $a_{\text{CDOM254}}$  stagnated until day 14, after which there

was a large drop in CDOM absorption (Fig. 5b). CDOM slope coefficient ( $S_{275-295}$ ) increased strongly during the first days of the spring experiment (Fig. 5c), but declined throughout the rest of the experiment. Changes in slope were modest in autumn (Fig. 5d), showing minor increase during the course of the experiment. Dynamics of the humic-like fluorescence was almost like an inverse of the CDOM slope, decreasing rapidly in the first few days of the spring experiment (Fig. 5e). Only minor changes were observed for the major part of the autumn experiment, except for the increase in the last days of the experiment (Fig. 5f). Protein-like fluorescence increased in the beginning of the spring experiment, and declined throughout the remaining of the experiment (Fig. 5g). The changes in protein-like fluorescence were more dynamic in the autumn experiment (Fig. 5h), but resulting in considerably lower levels at the end of the experiment compared to the initial conditions.

The repeated-measures mixed model approach revealed that season had a significant effect on the DOM characteristics, as there was a significant difference between spring and autumn for all 9 components from the PARAFAC analysis (Table 2). Also, season was a strong driver for the inorganic nitrogen and phosphorus concentrations. Further, experiment day had a significant effect on study variables, whereas the combined effect of treatment and experiment day was significant only for a few variables.

Principal component analysis (PCA) revealed temporal shifts in DOM characteristics (Fig. 6). In the spring experiment, the temporal changes along the PC axes were overall larger than in autumn in both CDOM spectral absorbance (Fig. 6a) and PARAFAC components (Fig. 6b). The largest excursions from initial conditions occurred in the early stage of the spring experiment. On the other hand, relatively small changes took place in the autumn experiment during the first two weeks; the largest change occurring between days 14 and 18. For CDOM spectral absorbance, the variation in eigenvectors across the wavelengths were minimal on PC1 (Fig. 6c), but highly dynamic for PC2 and PC3. This featureless shape of the eigenvectors of PC1 suggest that it is merely an indicator of the overall quantity of CDOM. Thus, we chose PC2 and PC3 to describe the spectral changes in CDOM absorbance during the experiments (Fig. 6a). During the first part of the experiment, the changes along PC2 axis were positive, resulting from increasing CDOM absorbance in wavelengths below 350 nm, and/or decreasing above (Fig. 6c). In the latter part of the experiments, this change was in inverse direction. Relative decrease in CDOM absorbance at wavelengths between 290 and 390 nm was driving the observed increase along the PC3 during the first days in spring.

Relative increase in this wavelength range resulted in decreases in PC3 on the latter part of the spring experiment, and throughout the autumn experiment. The variation among fluorescence components could, to large extent, be explained with the five humic-like components (C1–C4 and C6) and one protein-like component (C5). A large drop in these humic-like components was observed at day 4 in the spring experiment, but this change was almost reversed at day 7 although with a shift towards relatively higher C3 and C5 (Fig. 6b). However, these two components decreased towards the end of the spring experiment, returning to fluorescence composition similar to initial condition. Changes over time during the autumn experiments were of smaller magnitude, mostly dominated by a decreased in the protein-like C5. During spring experiment, the time trajectories of both spectral CDOM absorbance (Fig. 6a) and PARAFAC components (Fig. 6b) ended up relatively close to the initial (day 0) values, whereas in the autumn experiment the deviation from the initial conditions increased continuously throughout the experiment.

#### 4. Discussion

Availability of both nitrogen and phosphorus is a major driver of phytoplankton growth and the trophic state of coastal systems (Conley et al. 2009; Staehr et al. 2017). This was exemplified in our experiments in the negligible response of the Chl  $\alpha$  to nitrate additions in the spring experiment where inorganic nitrogen was readily available. Instead phytoplankton growth was limited by available phosphorus, decreasing to a level below 0.3–0.4  $\mu\text{mol l}^{-1}$  during the first days of the experiment. On the other hand, in the autumn experiment the phytoplankton community was obviously limited by nitrogen availability, as the nitrate additions induced a 3-fold increase in Chl  $\alpha$  concentration compared to control units with no nitrogen amendment. In general, the observed declines of the Chl  $\alpha$  in the experiments were likely driven by a combination of increasing grazing pressure by ciliates and other small grazers (Lampert et al. 1986) and depletion of key resource(s) (Hecky & Kilham 1988).

In our experiments, the phytoplankton community was dominated by the same major taxonomical groups in both spring and autumn (cryptophytes and diatoms), suggesting that the large differences in DOM dynamics and bioavailability were not directly linked to group-specific phytoplankton ER. Instead, we observed considerable differences in nutrient and DOM dynamics between the seasons, suggesting more complex suite of drivers than only

phytoplankton community composition. We argue that observed differences arose from a combination of the quality of the initial DOM pool and the nutrient limitation patterns.

DOM quantity and characteristics typically have intra-annual seasonal pattern in temperate coastal waters (Keith et al. 2002; Markager et al. 2011). In general, coastal DOM in spring has more pronounced terrestrial signal resulting from relatively high freshwater inputs draining the landscape and lower level of processing. In contrast, in autumn DOM has lesser terrestrial signal and has been processed further within the system, resulting in less bioavailable DOM (Wiegner et al. 2004; Stedmon et al. 2006). This seasonal variation in the bulk DOM was confirmed by our experiments, as the autumn DOM pool had initially weaker terrestrial signal, which suggests reduced terrestrial influence and increased processing by heterotrophs (Huguet et al. 2009; Asmala et al. 2013).

Heterotrophic microbes are not just consumers of DOM, but they are also known to transform non-colored DOM to colored DOM (Rochelle-Newall & Fisher 2002; Romera-Castillo et al. 2011). The emerging view is that the biological availability of DOM is not only a result of the inherent properties of the DOM pool, but a combination of the functioning of the bacterial community and environmental conditions, such as inorganic nutrient availability (Marín-Spiotta et al. 2014). Inorganic nutrient availability, especially phosphate, enhances bacterial DOM utilization (Kragh et al. 2008). On the other hand, nutrient availability also affects the growth and DOM release by phytoplankton (Mykkestad 1995; Klausmeier et al. 2004). This nutrient dependency is reflected in the amount of accumulated DOC, which was three times higher in N-limited autumn. Normalized to averaged Chl  $\alpha$ , this difference is even more pronounced, as in the autumn experiment the chlorophyll-specific increase in DOC was 14 times higher than in the spring experiment. This is likely the result of a more optimal phytoplankton growth in spring due to the replete available nitrogen (Klausmeier et al. 2004).

Despite the large seasonal differences in the amount of ER, the proportion of bioavailable DOC (BDOC) was relatively invariable; 13–18 % in both seasons. This proportion is surprisingly low, as in general, the average proportion of BDOC is 19% of the bulk DOC in marine environments (Søndergaard & Middelboe 1995) and traditionally, DOC originating from phytoplankton is considered to be more labile than the bulk DOC (Kirchman & Suzuki 1991; Chen & Wangersky 1996). As bacterial bioassays were spiked with abundant DIN and DIP, the low BDOC values suggest relatively poor quality of the accumulated DOC. This in

turn indicates rapid processing of ER already within the main incubations, where the most labile DOC fractions are already utilized prior to the BDOC bioassays.

Under replete inorganic nutrient conditions, bacteria may change their DOM utilization patterns towards more refractory CDOM with high C:N and C:P ratios, but with higher energy content (Asmala et al. 2014). Accumulation of CDOM followed opposite patterns compared to DOC, as there was an increase from the initial background values throughout the absorption spectrum in spring, consistent with DOC, and oppositely a CDOM decrease in autumn. This suggests that with P-limitation in spring, bacteria were either not able to utilize the phytoplankton derived CDOM, or they transformed the autochthonous non-colored DOM to CDOM. On the other hand, the abundant DIP in autumn allowed bacteria to utilize CDOM more effectively. Under conditions with low inorganic P and relatively labile bulk DOM, low-quality (high C to N/P ratio) autochthonous DOM is less favorable for heterotrophic consumption than the relatively fresh allochthonous DOM. On the other hand, high inorganic P and relatively refractory bulk DOM could stimulate bacterial processing of fresh autochthonous, but potentially nutrient-poor DOM. This difference in bacterial DOM source utilization is apparent in Fig. 2, which suggests that bacteria are able to utilize colored DOM when the availability of phosphorus is high.

Aquatic bacteria are transforming the DOM pool constantly by dissolution of particulates, direct uptake, extracellular release and respiration (Guillemette & del Giorgio 2012). Assessing the temporal changes in the DOM pool shows that the transformations are more dynamic than what can be captured by just comparing start and end of the experiments. The large decrease in humic-like fluorescence and molecular weight of DOM (as indicated by  $S_{275-295}$ ) in the first days of the spring experiment suggests that in the initial DOM pool there was large potential for bacterial utilization of fresh allochthonous material (Asmala et al. 2013). After the consumption of the labile DOM, the system shifts into more balanced production and consumption of DOM, as no large changes occur after day 4. In autumn, the temporal changes in DOM characteristics are relatively smaller compared to spring, apart from the end of the experiment where major changes in DOM characteristics coinciding with increases in DIN and DIP indicate remineralization of particulate matter to dissolved phase (Kragh & Søndergaard 2009). To overcome the apparent complexity in the temporal dynamics of DOM characteristics, we used multivariate analyses to follow the DOM transformation by analyzing the temporal changes in the spectral CDOM absorption and

fluorescent DOM components. It is evident that different regions of the CDOM absorption spectrum or different FDOM components contribute differently to the composition of the DOM pool depending on the biological drivers within the system.

As the absorption and fluorescence characteristics of DOM are tightly linked to its composition (Osburn & Bianchi 2016), it can be assumed that the observed changes reflect chemical transformation of the DOM pool. This transformation is a result of biogeochemical processing of DOM that is not unidirectional with a common endpoint, but is a more dynamic set of processes that depend on various factors, such as initial DOM quality (Ruiz-González et al. 2015; Amaral et al. 2016), metabolism of the bacterial community (Cammack et al. 2004; Logue et al. 2015; Kaartokallio et al. 2016) and inorganic nutrient status (Zweifel et al. 1993; Asmala et al. 2014). Interestingly, PCA revealed that in the spring experiment the DOM pool seemed to return to its original characteristics, similar to the background DOM. On the other hand, in autumn the transformations continuously increased in distance from the point of origin. Overall, the processing of the DOM pool was more dynamic in spring than in autumn, which agrees with the smaller changes in spectral CDOM absorption and higher net accumulation of DOC in autumn. This indicates lower degree of transformations in general to the DOM pool in autumn, likely due its poorer quality, excreted by N-limited phytoplankton. In autumn DOM is gradually transformed towards a more refractory state. In spring, combination of large, labile pool of allochthonous DOM and high phytoplankton production leads to more dynamic changes in the DOM pool, as the primary sources for the heterotrophic consumption change during the course of the experiment. This observed seasonal shift is likely the result in balance and availability of DIN and DIP, but also stoichiometry of organic nutrients (Bronk et al. 1998).

These findings show that the contribution of phytoplankton-derived DOM to the bulk DOM pool varies on a seasonal scale, and is strongly driven by inorganic nutrient availability and bulk DOM quality. It is still highly uncertain which are the heterotrophic pathways participating in the DOM transformation processes in the pelagic food web, and what are their major environmental drivers. Assessing with multiple quality proxies, DOM transformation by heterotrophic processes does not seem to follow a uniform path but follows a seasonally distinct temporal trajectories. The seasonal differences in available nitrogen and phosphorus alter the DOM processing pathways, as the DOM originating from phytoplankton differs depending on the nutrient conditions. In conditions where the extracellular release of

DOM from phytoplankton is of low quality, bacterial carbon demand may be fulfilled with the ambient DOM instead. Further, the prevailing nutrient conditions also affect the bacterial metabolism of phytoplankton-derived DOM, resulting in DOM pool shaped by the environmental controls.

## Acknowledgements

This study was supported by the BONUS COCOA project (grant agreement 2112932-1), funded jointly by the EU and Danish Research Council. The authors would like to thank Colin Stedmon (DTU Aqua, Denmark) for the DOC analysis. L.H. was supported by a grant from the Brazilian program Science without Borders/CAPES (Grant no. 13581-13-9). P.M. was supported by a postdoctoral fellowship from The Natural Sciences and Engineering Research Council of Canada (NSERC).

## References

- Aluwihare L, Repeta D (1999) A comparison of the chemical characteristics of oceanic DOM and extracellular DOM produced by marine algae. *Mar Ecol Prog Ser*:105-117
- Amaral V, Graeber D, Calliari D, Alonso C (2016) Strong linkages between DOM optical properties and main clades of aquatic bacteria. *Limnol Oceanogr* 61:906-918
- Asmala E, Autio R, Kaartokallio H, Stedmon CA, Thomas D (2014) Processing of humic-rich riverine dissolved organic matter by estuarine bacteria: effects of predegradation and inorganic nutrients. *Aquat Sci* 76:451
- Asmala E, Autio R, Kaartokallio H, Pitkänen L, Stedmon C, Thomas D (2013) Bioavailability of riverine dissolved organic matter in three Baltic Sea estuaries and the effect of catchment land use. *Biogeosciences* 10:6969-6986
- Boyd TJ, Osburn CL (2004) Changes in CDOM fluorescence from allochthonous and autochthonous sources during tidal mixing and bacterial degradation in two coastal estuaries. *Mar Chem* 89:189-210
- Bronk DA, Glibert PM, Malone TC, Banahan S, Sahlsten E (1998) Inorganic and organic nitrogen cycling in Chesapeake Bay: autotrophic versus heterotrophic processes and relationships to carbon flux. *Aquat Microb Ecol* 15:177-189
- Cammack W, Kalff J, Prairie YT, Smith EM (2004) Fluorescent dissolved organic matter in lakes: relationships with heterotrophic metabolism. *Limnol Oceanogr* 49:2034-2045

436 Carlson CA, Hansell DA (2014) DOM sources, sinks, reactivity, and budgets. In:  
 437 Biogeochemistry of Marine Dissolved Organic Matter: Second Edition. Elsevier Inc.  
 438 Chen W, Wangersky PJ (1996) Rates of microbial degradation of dissolved organic carbon  
 439 from phytoplankton cultures. *J Plankton Res* 18:1521-1533  
 440 Coble PG (1996) Characterization of marine and terrestrial DOM in seawater using  
 441 excitation-emission matrix spectroscopy. *Mar Chem* 51:325-346  
 442 Conley DJ, Paerl HW, Howarth RW, Boesch DF, Seitzinger SP, Havens KE, Lancelot C,  
 443 Likens GE (2009) Controlling eutrophication: nitrogen and phosphorus. *Science*  
 444 Dainard PG, Guéguen C, McDonald N, Williams WJ (2015) Photobleaching of fluorescent  
 445 dissolved organic matter in Beaufort Sea and North Atlantic Subtropical Gyre. *Mar Chem*  
 446 177:630-637  
 447 Danhiez F, Vantrepotte V, Cauvin A, Lebourg E, Loisel H (2017) Optical properties of  
 448 chromophoric dissolved organic matter during a phytoplankton bloom. Implication for DOC  
 449 estimates from CDOM absorption. *Limnol Oceanogr*  
 450 Flindt MR, Kamp-Nielsen L, Marques JC, Pardal MA, Bocci M, Bendoricchio G,  
 451 Salomonsen J, Nielsen SN, Jørgensen SE (1997) Description of the three shallow estuaries:  
 452 Mondego River (Portugal), Roskilde Fjord (Denmark) and the lagoon of Venice (Italy). *Ecol*  
 453 *Model* 102:17-31  
 454 Graeber D, Gelbrecht J, Pusch MT, Anlanger C, von Schiller D (2012) Agriculture has  
 455 changed the amount and composition of dissolved organic matter in Central European  
 456 headwater streams. *Sci Total Environ* 438:435-446  
 457 Guillemette F, del Giorgio PA (2012) Simultaneous consumption and production of  
 458 fluorescent dissolved organic matter by lake bacterioplankton. *Environ Microbiol* 14:1432-  
 459 1443  
 460 Hansen HP, Koroleff F (2007) Determination of nutrients. *Methods of Seawater Analysis*,  
 461 Third Edition:159-228  
 462 Hasle G (1978) The inverted microscope method. *Phytoplankton manual*  
 463 He XS, Xi BD, Gao RT, Wang L, Ma Y, Cui DY, Tan WB (2015) Using fluorescence  
 464 spectroscopy coupled with chemometric analysis to investigate the origin, composition, and  
 465 dynamics of dissolved organic matter in leachate-polluted groundwater. *Environ Sci Pollut*  
 466 *Res Int* 22:8499-8506  
 467 Holm-Hansen O, Riemann B (1978) Chlorophyll a determination: improvements in  
 468 methodology. *Oikos*



469 Jørgensen L, Stedmon CA, Kragh T, Markager S, Middelboe M, Søndergaard M (2011)  
 470 Global trends in the fluorescence characteristics and distribution of marine dissolved organic  
 471 matter. *Mar Chem* 126:139-148  
 472 Kaartokallio H, Asmala E, Autio R, Thomas DN (2016) Bacterial production, abundance and  
 473 cell properties in boreal estuaries: relation to dissolved organic matter quantity and quality.  
 474 *Aquat Sci* 78:525-540  
 475 Keith D, Yoder J, Freeman S (2002) Spatial and temporal distribution of coloured dissolved  
 476 organic matter (CDOM) in Narragansett Bay, Rhode Island: implications for phytoplankton  
 477 in coastal waters. *Estuar Coast Shelf Sci* 55:705-717  
 478 Kirchman DL, Suzuki Y (1991) High turnover rates of dissolved organic carbon during a  
 479 spring phytoplankton bloom. *Nature* 352:612  
 480 Klausmeier CA, Litchman E, Daufresne T, Levin SA (2004) Optimal nitrogen-to-phosphorus  
 481 stoichiometry of phytoplankton. *Nature* 429:171-174  
 482 Kothawala DN, von Wachenfeldt E, Koehler B, Tranvik LJ (2012) Selective loss and  
 483 preservation of lake water dissolved organic matter fluorescence during long-term dark  
 484 incubations. *Sci Total Environ* 433:238-246  
 485 Kragh T, Søndergaard M (2009) Production and decomposition of new DOC by marine  
 486 plankton communities: carbohydrates, refractory components and nutrient limitation.  
 487 *Biogeochemistry* 96:177-187  
 488 Kragh T, Søndergaard M, Tranvik L (2008) Effect of exposure to sunlight and phosphorus-  
 489 limitation on bacterial degradation of coloured dissolved organic matter (CDOM) in  
 490 freshwater. *FEMS Microbiol Ecol* 64:230-239  
 491 Lambert T, Bouillon S, Darchambeau F, Massicotte P, Borges AV (2016) Shift in the  
 492 chemical composition of dissolved organic matter in the Congo River network.  
 493 *Biogeosciences* 13:5405  
 494 Lampert W, Fleckner W, Rai H, Taylor BE (1986) Phytoplankton control by grazing  
 495 zooplankton: a study on the spring clear-water phase. *Limnol Oceanogr* 31:478-490  
 496 Li Zweifel U, Norrman B, Hagström Å (1993) Consumption of dissolved organic carbon by  
 497 marine bacteria and demand for inorganic nutrients. *Mar Ecol Prog Ser*:23-32  
 498 Logue JB, Stedmon CA, Kellerman AM, Nielsen NJ, Andersson AF, Laudon H, Lindström  
 499 ES, Kritzberg ES (2016) Experimental insights into the importance of aquatic bacterial  
 500 community composition to the degradation of dissolved organic matter. *The ISME journal*  
 501 10:533-545

502 Marín-Spiotta E, Gruley K, Crawford J, Atkinson E, Miesel J, Greene S, Cardona-Correa C,  
 503 Spencer M (2014) Paradigm shifts in soil organic matter research affect interpretations of  
 504 aquatic carbon cycling: transcending disciplinary and ecosystem boundaries.  
 505 Biogeochemistry 117:279  
 506 Markager S, Stedmon CA, Søndergaard M (2011) Seasonal dynamics and conservative  
 507 mixing of dissolved organic matter in the temperate eutrophic estuary Horsens Fjord. Estuar  
 508 Coast Shelf Sci 92:376-388  
 509 Moran MA, Sheldon WM, Zepp RG (2000) Carbon loss and optical property changes during  
 510 long-term photochemical and biological degradation of estuarine dissolved organic matter.  
 511 Limnol Oceanogr 45:1254-1264  
 512 Murphy KR, Stedmon CA, Graeber D, Bro R (2013) Fluorescence spectroscopy and multi-  
 513 way techniques. PARAFAC. Analytical Methods 5:6557-6566  
 514 Murphy KR, Hambly A, Singh S, Henderson RK, Baker A, Stuetz R, Khan SJ (2011)  
 515 Organic matter fluorescence in municipal water recycling schemes: toward a unified  
 516 PARAFAC model. Environ Sci Technol 45:2909-2916  
 517 Murphy KR, Butler KD, Spencer RG, Stedmon CA, Boehme JR, Aiken GR (2010)  
 518 Measurement of dissolved organic matter fluorescence in aquatic environments: an  
 519 interlaboratory comparison. Environ Sci Technol 44:9405-9412  
 520 Murphy KR, Stedmon CA, Waite TD, Ruiz GM (2008) Distinguishing between terrestrial  
 521 and autochthonous organic matter sources in marine environments using fluorescence  
 522 spectroscopy. Mar Chem 108:40-58  
 523 Murphy KR, Ruiz GM, Dunsmuir WT, Waite TD (2006) Optimized parameters for  
 524 fluorescence-based verification of ballast water exchange by ships. Environ Sci Technol  
 525 40:2357-2362  
 526 Mykkestad SM (1995) Release of extracellular products by phytoplankton with special  
 527 emphasis on polysaccharides. Sci Total Environ 165:155-164  
 528 Osburn CL, Bianchi TS (2016) Linking optical and chemical properties of dissolved organic  
 529 matter in natural waters. Frontiers in Marine Science 3:223  
 530 Osburn CL, Stedmon CA (2011) Linking the chemical and optical properties of dissolved  
 531 organic matter in the Baltic–North Sea transition zone to differentiate three allochthonous  
 532 inputs. Mar Chem 126:281-294  
 533 Reader HE, Stedmon CA, Nielsen NJ, Kritzberg ES (2015) Mass and UV-visible spectral  
 534 fingerprints of dissolved organic matter: sources and reactivity. Frontiers in Marine Science  
 535 2:88

536 Rochelle-Newall E, Fisher T (2002) Production of chromophoric dissolved organic matter  
 537 fluorescence in marine and estuarine environments: an investigation into the role of  
 538 phytoplankton. *Mar Chem* 77:7-21  
 539 Romera-Castillo C, Sarmento H, Alvarez-Salgado XA, Gasol JM, Marrase C (2011) Net  
 540 production and consumption of fluorescent colored dissolved organic matter by natural  
 541 bacterial assemblages growing on marine phytoplankton exudates. *Appl Environ Microbiol*  
 542 77:7490-7498  
 543 Ruiz-González C, Niño-García JP, Lapierre J, del Giorgio PA (2015) The quality of organic  
 544 matter shapes the functional biogeography of bacterioplankton across boreal freshwater  
 545 ecosystems. *Global Ecol Biogeogr* 24:1487-1498  
 546 Sarmento H, Romera-Castillo C, Lindh M, Pinhassi J, Sala MM, Gasol JM, Marrasé C,  
 547 Taylor GT (2013) Phytoplankton species-specific release of dissolved free amino acids and  
 548 their selective consumption by bacteria. *Limnol Oceanogr* 58:1123-1135  
 549 Shutova Y, Baker A, Bridgeman J, Henderson RK (2014) Spectroscopic characterisation of  
 550 dissolved organic matter changes in drinking water treatment: from PARAFAC analysis to  
 551 online monitoring wavelengths. *Water Res* 54:159-169  
 552 Søndergaard M, Williams, Peter J le B, Cauwet G, Riemann B, Robinson C, Terzic S,  
 553 Woodward EMS, Worm J (2000) Net accumulation and flux of dissolved organic carbon and  
 554 dissolved organic nitrogen in marine plankton communities. *Limnol Oceanogr* 45:1097-1111  
 555 Søndergaard M, Middelboe M (1995) A cross-system analysis of labile dissolved organic  
 556 carbon. *Mar Ecol Prog Ser*:283-294  
 557 Staehr PA, Testa J, Carstensen J (2017) Decadal Changes in Water Quality and Net  
 558 Productivity of a Shallow Danish Estuary Following Significant Nutrient Reductions.  
 559 *Estuaries and Coasts* 40:63-79  
 560 Stedmon CA, Thomas DN, Papadimitriou S, Granskog MA, Dieckmann GS (2011) Using  
 561 fluorescence to characterize dissolved organic matter in Antarctic sea ice brines. *Journal of*  
 562 *Geophysical Research: Biogeosciences* 116  
 563 Stedmon CA, Thomas DN, Granskog M, Kaartokallio H, Papadimitriou S, Kuosa H (2007)  
 564 Characteristics of dissolved organic matter in Baltic coastal sea ice: allochthonous or  
 565 autochthonous origins?. *Environ Sci Technol* 41:7273-7279  
 566 Stedmon CA, Markager S, Søndergaard M, Vang T, Laubel A, Borch NH, Windelin A (2006)  
 567 Dissolved organic matter (DOM) export to a temperate estuary: seasonal variations and  
 568 implications of land use. *Estuaries and Coasts* 29:388-400

Stedmon CA, Markager S (2005) Resolving the variability in dissolved organic matter fluorescence in a temperate estuary and its catchment using PARAFAC analysis. *Limnol Oceanogr* 50:686-697

Stedmon CA, Markager S, Bro R (2003) Tracing dissolved organic matter in aquatic environments using a new approach to fluorescence spectroscopy. *Mar Chem* 82:239-254

Thornton DC (2014) Dissolved organic matter (DOM) release by phytoplankton in the contemporary and future ocean. *Eur J Phycol* 49:20-46

Utermöhl H (1958) Zur vervollkommnung der quantitativen phytoplankton methodik

Vähätalo AV, Aarnos H, Mäntyniemi S (2010) Biodegradability continuum and biodegradation kinetics of natural organic matter described by the beta distribution. *Biogeochemistry* 100:227-240

Walker SA, Amon RM, Stedmon C, Duan S, Louchouart P (2009) The use of PARAFAC modeling to trace terrestrial dissolved organic matter and fingerprint water masses in coastal Canadian Arctic surface waters. *Journal of Geophysical Research: Biogeosciences* 114

Weishaar JL, Aiken GR, Bergamaschi BA, Fram MS, Fujii R, Mopper K (2003) Evaluation of specific ultraviolet absorbance as an indicator of the chemical composition and reactivity of dissolved organic carbon. *Environ Sci Technol* 37:4702-4708

Wiegner TN, Seitzinger SP (2004) Seasonal bioavailability of dissolved organic carbon and nitrogen from pristine and polluted freshwater wetlands. *Limnol Oceanogr* 49:1703-1712

Yamashita Y, Boyer JN, Jaffe R (2013) Evaluating the distribution of terrestrial dissolved organic matter in a complex coastal ecosystem using fluorescence spectroscopy. *Cont Shelf Res* 66:136-144

Yamashita Y, Kloeppel BD, Knoepp J, Zausen GL, Jaffé R (2011) Effects of watershed history on dissolved organic matter characteristics in headwater streams. *Ecosystems* 14:1110-1122

Yamashita Y, Tanoue E (2004) In situ production of chromophoric dissolved organic matter in coastal environments. *Geophys Res Lett* 31

Zsolnay A, Baigar E, Jimenez M, Steinweg B, Saccomandi F (1999) Differentiating with fluorescence spectroscopy the sources of dissolved organic matter in soils subjected to drying. *Chemosphere* 38:45-50

## Figures

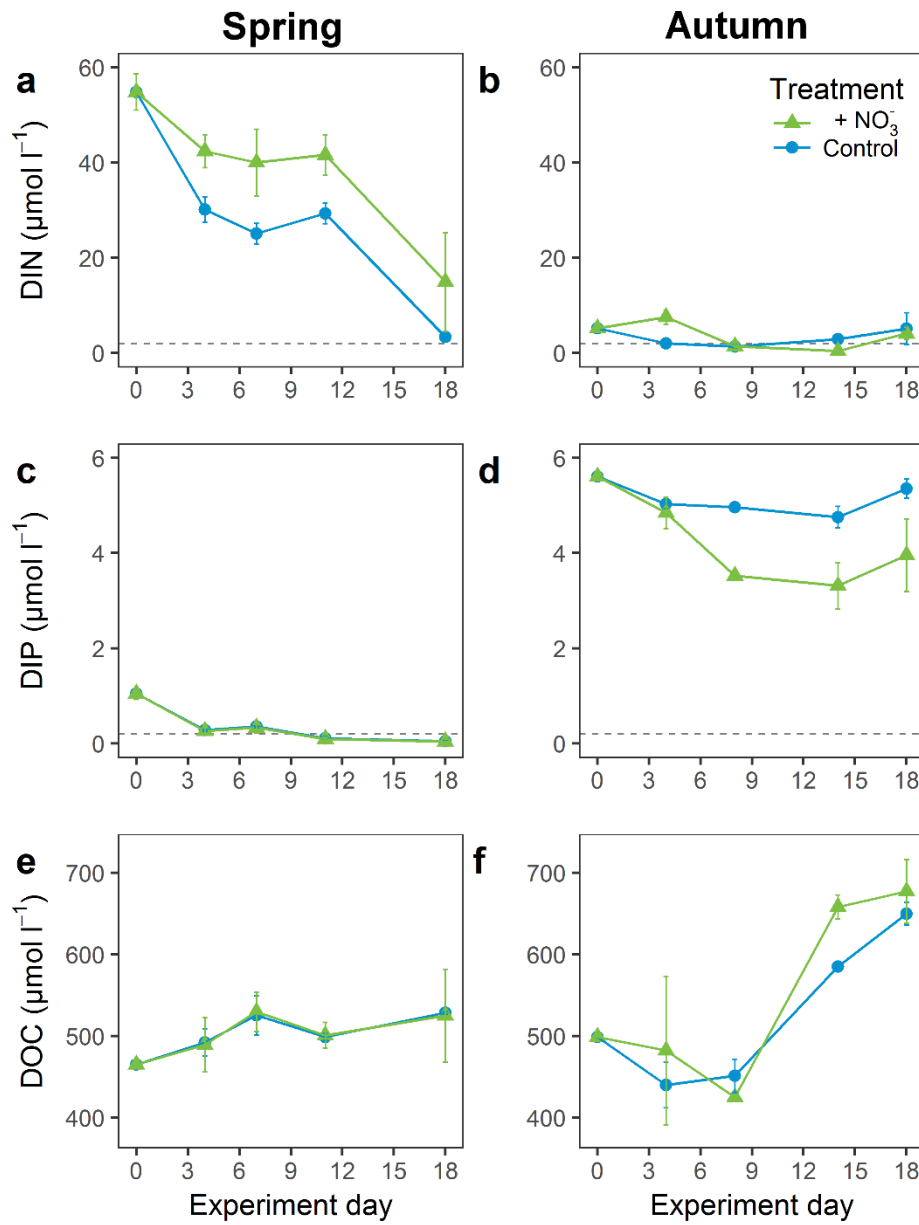


Fig. 1. Dynamics of DIN, DIP and DOC during the 18-d incubations in spring, and autumn experiments. Data points are average values from replicate units ( $n = 3$ ) for both treatments, error bars indicate one standard deviation among the replicate units. Gray dashed lines in a-b and c-d indicate levels of potential DIN and DIP limitation ( $2$  and  $0.2 \mu\text{mol l}^{-1}$ , respectively).

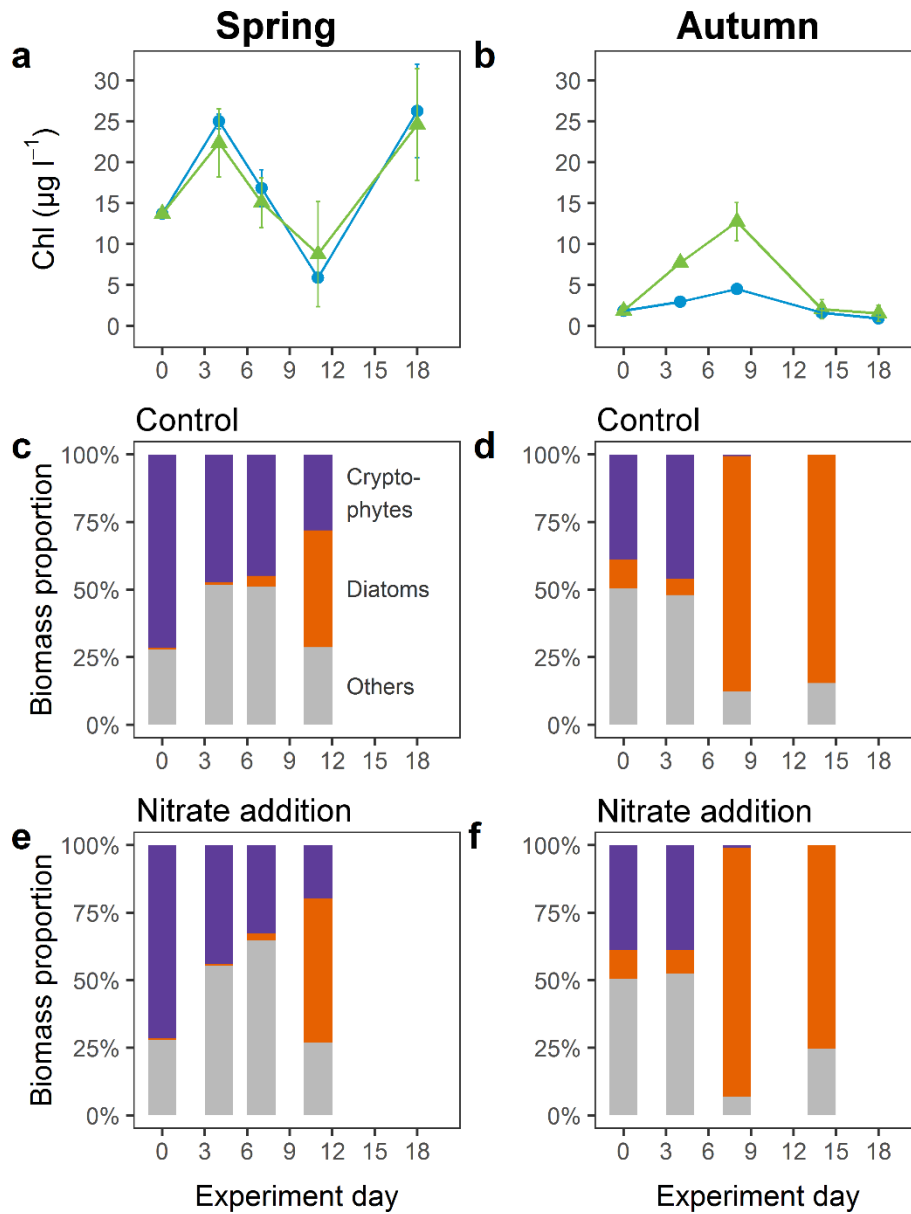


Fig. 2. Dynamics of phytoplankton biomass (as indicated by average ( $n = 3$ ) chlorophyll  $\alpha$  concentrations, a–b) and phytoplankton community composition (as indicated by the average ( $n = 3$ ) proportion of the major groups of the total biomass, c–f) during the experiments.

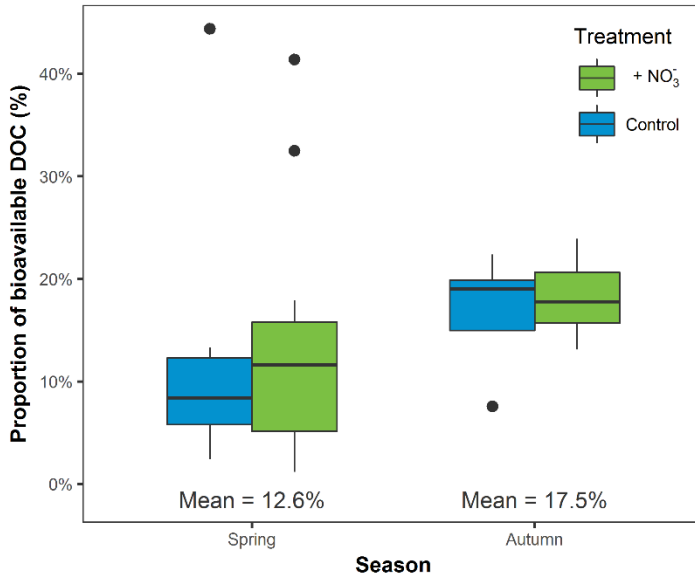


Fig. 3. Proportion of the bioavailable DOC (BDOC) during the experiments. Nutrient additions had no significant effect on the amount of BDOC ( $p = 0.577$  and  $0.715$  for spring and autumn, respectively), whereas season had a significant effect ( $p = 0.003$ ).

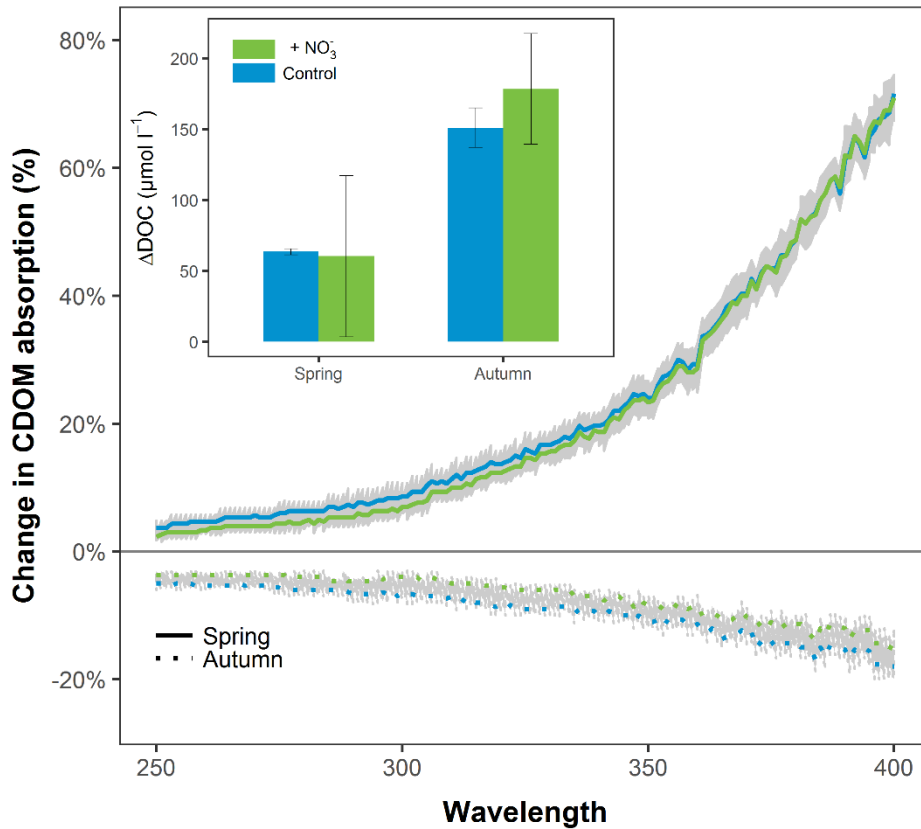


Fig. 4. Changes in the colored fraction of the DOM pool during the 18-d experiments. Lines show the relative changes from experiment start to end in spectral CDOM absorbance in spring and autumn. Lines are mean values of replicate units ( $n = 3$ ), and the gray shaded

ribbons mark one standard deviation. Bars show the net change in DOC concentration ( $\Delta\text{DOC}$ ) during the incubations. Each bar is the mean value of replicate units ( $n = 3$ ).

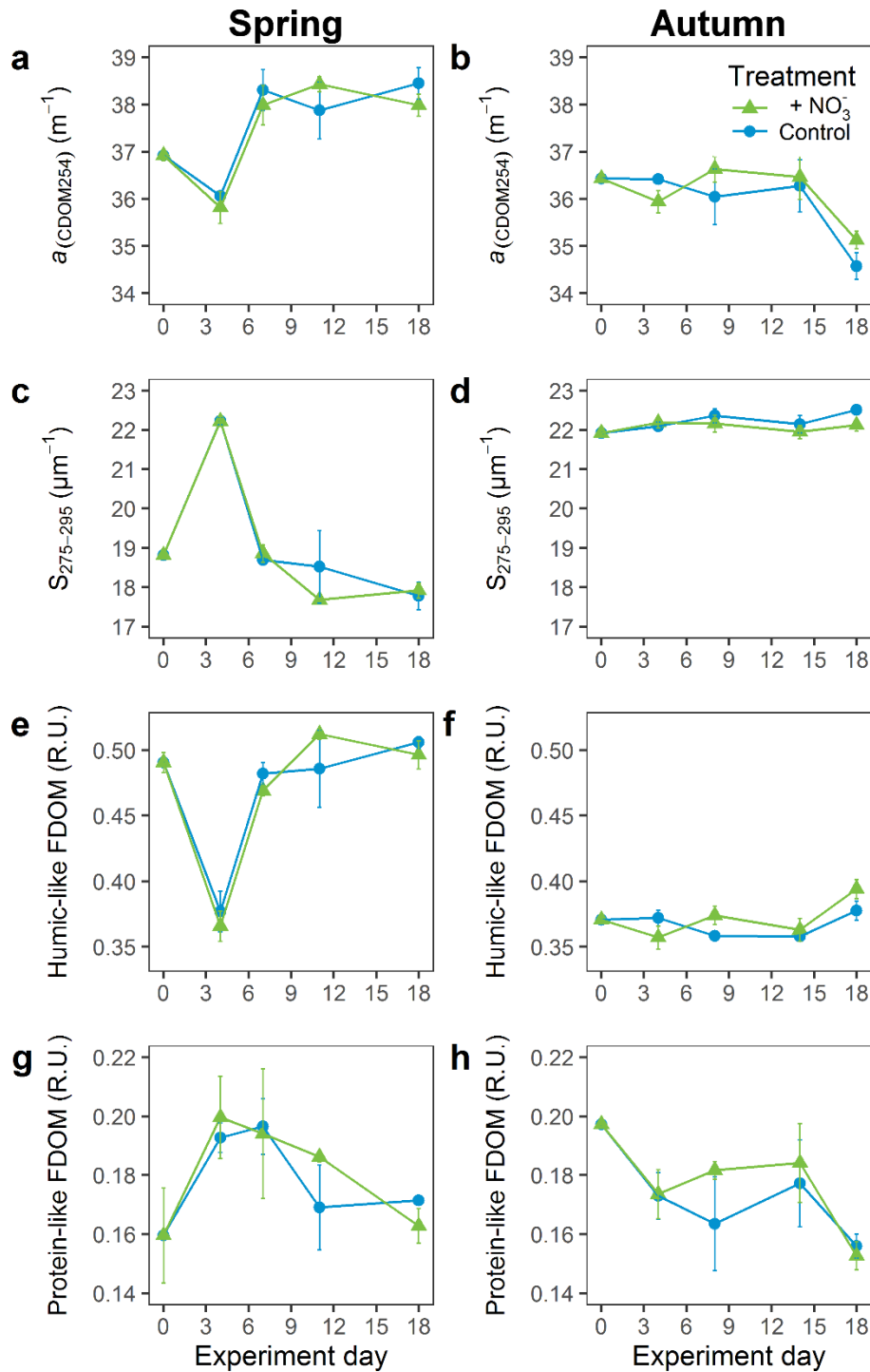


Fig. 5. DOM dynamics during the two experiments: a–b; CDOM absorption at 254 nm ( $a_{(\text{CDOM}_{254})}$ ), c–d; absorption slope between 275–295 nm ( $S_{275-295}$ ), e–f; humic-like fluorescence (Peak C; Coble 1996) and g–h; protein-like fluorescence (Peak T; Coble 1996).



Data points are average values from replicate units ( $n = 3$ ) for both treatments, error bars indicate one standard deviation among the replicate units.

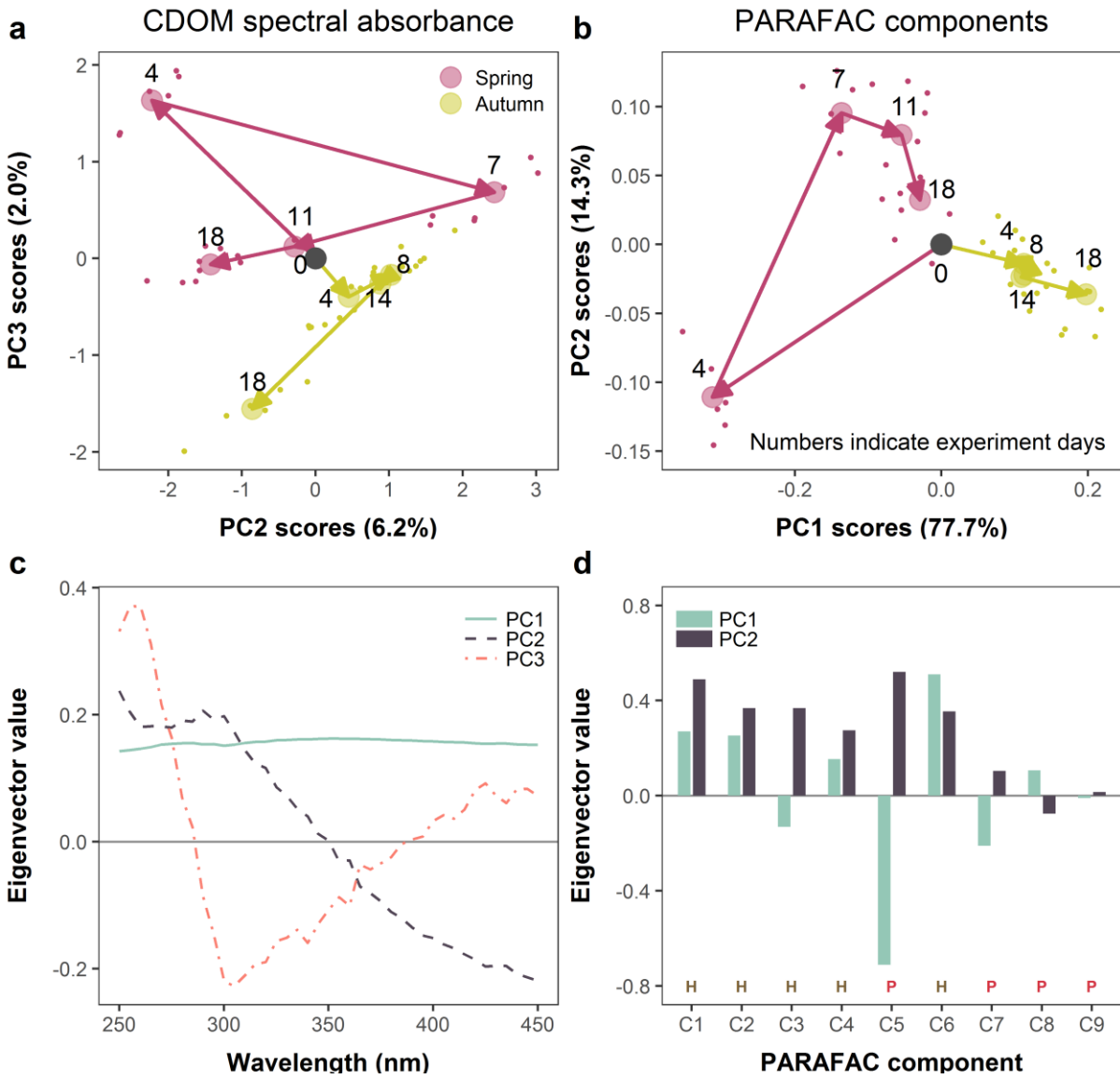


Fig. 6. Results of the principal component analysis (PCA) of spectral CDOM absorbance (a, c) and the 9 PARAFAC components (b, d). PCA was carried out with observations normalized to initial conditions, making the two experiments directly comparable. Upper panels (a, b) are biplots of two principal components (PC2 and PC3 for spectral CDOM absorbance, PC1 and PC2 for the components). Small points indicate individual observations, and large, numbered points daily means of (a) absorbance spectra and (b) PARAFAC components ( $n = 6$ ). Arrows show the time trajectories for the two seasons (labeled with day number) starting at the same normalized condition (day 0), marked with a black circle. Lower panels show eigenvectors of the PC's along the absorption spectrum (c) and across the 9

PARAFAC components (d). PARAFAC components in panel (d) are labeled with H (humic-like) or P (protein-like).

## Tables

Table 1. Initial DOM characteristics of the two experiments. DOC = dissolved organic carbon,  $a_{\text{CDOM}254}$  = CDOM absorption coefficient at 254 nm,  $a_{\text{CDOM}440}$  = CDOM absorption coefficient at 440 nm,  $\text{SUVA}_{254}$  = DOC-specific absorbance at 254 nm (Weishaar et al. 2003),  $S_{275-295}$  = CDOM spectral slope coefficient between 275 and 295 nm, Peak T = protein-like DOM fluorescence (Coble 1996), Peak C = humic-like DOM fluorescence (Coble 1996), HIX = DOM humification index (Zsolnay et al. 1999) and BIX = biological index (Huguet et al. 2009).

Variable	Spring	Autumn
DOC ( $\mu\text{mol l}^{-1}$ )	465	499
$a_{\text{CDOM}254}$ ( $\text{m}^{-1}$ )	38.9	36.4
$a_{\text{CDOM}440}$ ( $\text{m}^{-1}$ )	2.58	2.30
$\text{SUVA}_{254}$ ( $\text{m}^2 \text{g}^{-1} \text{C}$ )	3.03	2.64
$S_{275-295}$ ( $\mu\text{m}^{-1}$ )	18.8	21.9
Protein-like peak T (R.U.)	0.16	0.20
Humic-like peak C (R.U.)	0.49	0.37
HIX	15.0	9.87
BIX	0.67	0.74

Table 2. P values of the repeated measures mixed model showing the significance of season, treatment, experiment day and their combination in observed changes in selected study variables. Significant ( $P < 0.05$ ) values are marked in bold.

Variable	Season	Treatment	Season × Treatment	Experiment day (seasons separated)	Treatment × Experiment day (seasons separated)
DIN	<b>&lt;0.0001</b>	<b>0.0006</b>	<b>0.0010</b>	<b>&lt;0.0001</b>	0.6515
DIP	<b>0.0337</b>	<b>0.0010</b>	<b>0.0012</b>	<b>&lt;0.0001</b>	<b>0.0004</b>
Chl $\alpha$	0.1434	0.2954	0.1144	<b>&lt;0.0001</b>	0.1039
DOC	0.9500	0.2398	0.2327	<b>&lt;0.0001</b>	0.3719
C1	<b>&lt;0.0001</b>	0.1563	0.8329	<b>&lt;0.0001</b>	<b>0.0133</b>
C2	<b>&lt;0.0001</b>	0.3968	0.2424	<b>&lt;0.0001</b>	<b>0.0166</b>
C3	<b>0.0001</b>	0.5475	0.2619	<b>0.0010</b>	0.2761
C4	<b>&lt;0.0001</b>	0.3807	0.1341	<b>&lt;0.0001</b>	<b>0.0021</b>
C5	<b>&lt;0.0001</b>	0.4176	0.6275	<b>&lt;0.0001</b>	0.2701
C6	<b>&lt;0.0001</b>	0.5265	0.3743	<b>&lt;0.0001</b>	0.3137
C7	<b>&lt;0.0001</b>	0.9998	0.4739	<b>&lt;0.0001</b>	0.2813
C8	<b>&lt;0.0001</b>	0.2171	0.9433	<b>0.0022</b>	0.2710
C9	<b>0.0032</b>	0.5186	0.6487	<b>0.0005</b>	0.6573

656

657